

A frequency stabilized waveguide CO₂-laser for photoacoustic spectroscopy of gases*

GORDANA M. OSTOJIĆ, BOJAN B. RADAK and LJUBICA T. PETKOVSKA

*Vinča Institute of Nuclear Sciences, Department of Physical Chemistry, P.O. Box 522, YU-11001
Belgrade, Yugoslavia*

(Received 27 October 1999, revised 25 February 2000)

A theoretical model of a waveguide CO₂-laser was made to optimize the dimensions of the waveguide tube and resonator, *i.e.*, to obtain the best mode structure while maximizing the output power. The results were used to design and build the laser itself around a quartz waveguide tube of 25.5 cm and 3 mm inner diameter. A simple, low-cost, and efficient VMOS based current stabilization was applied, which stabilized the current to within ± 0.5 %. The working laser frequency selection and/or frequency stabilization was controlled by a piezo micro-positioner, which was coupled with an output power meter *via* a PC computer and driven by self-made software developed for the purpose. The experimental test of the laser showed good agreement with the model.

Keywords: CO₂-laser, photoacoustic spectroscopy, gases.

INTRODUCTION

Waveguide (WG) lasers have in practice become the most frequent type of mid- and low-power lasers used in spectroscopy. Although practical spectroscopic data can be obtained by classical non-tunable gas lasers too,¹⁻⁴ the main advantages of WG lasers over the corresponding classical devices working at lower gas pressures are: higher gain, broader emission lines, tuning capabilities within the broadened emission line, better mode structure, and small dimensions. This type of laser is very resistant to thermally induced mechanical instabilities of the resonator, providing at the same time high gains and saturation intensities. All of these characteristics ensure high power with respect to the active volume, as well as a stable output. Working pressures that range up to 150 mbar provide wide emission lines, and short resonator lengths provide tunability, obtainable *via* resonator length control. Both of these features make WG gas lasers especially applicable in spectroscopy.

The present paper describes the design and construction of a simple DC discharge excited waveguide CO₂-laser, with low-cost current stabilization and piezo-mechanical control of the resonator length.

The primary task of the present work was to determine the optimum dimensions of the WG tube and the resonator. A computer model of the laser was

* Dedicated to Professor Slobodan Ribnikar on the occasion of his 70th birthday.

developed, based on the known theory.⁵⁻⁸ For each set of dimensions as input, the model yields the losses of the four fundamental radially symmetric modes, as output. These losses are associated with introducing polarization elements (Brewster windows) and a rotating reflective grating. The free spaces between the WG tube and the terminal elements (mirror and grating) dissipate the optical power and mix the WG modes. We show, however, that a specific range of dimensions produces a local minimum of losses and provides a monomode output even while scanning across an emission line by varying the free spectral range of the resonator.

THE MODE COUPLING MODEL

Here the laser tube is considered to be a passive waveguide, without excitation, a hollow dielectric waveguide of circular cross-section in a Fabri-Perot resonator.^{5,6} Both TM and TE modes can propagate in a hollow waveguide, but since the laser has one intracavity Brewster window, a combination of degenerated modes is applied, such that it consists of a set of linearly polarized, radially symmetric, EH_{1p} modes. The propagation of the electric field of these modes inside the WG tube made with refractive index n_0 , and inner radius a , is defined by the following equation:

$$E_{1p}(r) = J_0 \left(\frac{U_{1p}r}{a} \right) \exp[j(\gamma z - \omega t)] \quad (1)$$

U_{1p} is the p -th root of the equation $J_0(U_{1p}) = 0$, where J_0 is a first order Bessel function, z is the coordinate in the direction of propagation, ω – the working laser frequency, and γ is the propagation constant of the mode defined by equation:

$$\gamma = k \left[1 - \frac{1}{2} \left(\frac{U_{1p}}{ka} \right)^2 \left(1 - j \frac{2n}{ka} \right) \right] \quad (2)$$

where $k = 2\pi/\lambda$ is the wavenumber, and j the imaginary unit. The constant n is associated with the dielectric constant of the WG tube material, n_0 (refractive index), and, for the hybrid EH modes, is defined as:

$$n = (n_0^2 + 1)/2\sqrt{n_0^2 - 1} \quad (3)$$

In the free space where the light leaves the WG tube the diffraction of the EH modes is observed through the propagation of the TEM_{m0} modes. Mode coupling occurs in such a way that the largest part of an EH_{1p} mode transforms into the $TEM_{p-1,0}$ mode outside the waveguide.

In order to calculate the losses in the whole resonator it is necessary to sum all the losses of each mode along the whole trip of a photon around the resonator. For this purpose the resonator can be substituted by an equivalent system, shown in Fig. 1.

The losses were calculated for 4 fundamental EH modes, while in the free space they are represented by 6 fundamental TEM modes. At the exit of the WG

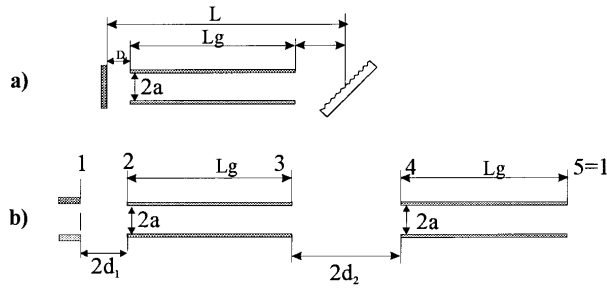


Fig. 1. Schematic presentation of the waveguide laser: a) the real resonator and b) the equivalent resonator schematic. The labels are: L = resonator length, L_g = waveguide tube length, d_1 = mirror-to-waveguide distance, d_2 = waveguide-to-grating distance, a = waveguide tube radius.

cavity (cross section plane 1, Fig. 1) EH modes transform into TEM modes. The transformation can be represented by a transformation matrix \mathbf{M}_1 . During further propagation along the part $2d_1$, the set of TEM modes undergoes a phase shift that can be represented by a square matrix \mathbf{M}_2 . The phase shifts of the waves, which depend on the longitudinal position, are first taken into account at the entrance into the WG tube and presented by matrix \mathbf{M}_3 . The latter matrix transforms TEM modes into EH modes in plane 2. Matrix \mathbf{M}_4 defines the changes of WG modes along the WG cavity. Mode propagation can be similarly presented for the other part of the free path, *i.e.*, for $2d_2$. Naturally, since the distance is different, there will be matrix \mathbf{M}_5 instead of \mathbf{M}_2 , and \mathbf{M}_6 instead of \mathbf{M}_3 . In this way, the whole round-trip of the waveguide modes can be represented by matrix \mathbf{M} , defined by:

$$\mathbf{M} = \mathbf{M}_4 \mathbf{M}_6 \mathbf{M}_5 \mathbf{M}_1 \mathbf{M}_4 \mathbf{M}_3 \mathbf{M}_2 \mathbf{M}_1 \quad (4)$$

The losses of the EH_{1p} mode are given as:

$$L_{1p} = 1 - \text{abs}(L_p)^2 \quad (5)$$

where L_p are eigen values of matrix \mathbf{M} .

The analysis can be broadened by introducing other sets of linearly polarized modes, but these are significant only as a secondary effect. Since the mode EH_{11} has the lowest losses, its coupling with other radially symmetric EH_{1p} modes is most significant for the calculation.

MODELING RESULTS

The main purpose of the above theoretical model was to serve as the basis for the design of a real laser. In reality, however, there are several basic limitations for the dimensions of the laser. The diffraction grating that selects the emission lines requires the beam diameter to be at least 2.8 mm for efficient line selection. Thus, an inner diameter of 3 mm was chosen for the WG tube. The theory also showed that an asymmetrical resonator is preferable to a symmetric one, requiring the mirror-to-waveguide distance to be as small as possible, since the grating-to-waveguide distance needed to be larger. In our case, a sustainable construction

required a minimal distance of $d_1=23$ mm. The limitations partly include the length of the active volume, *i.e.*, the WG tube itself. In order for the laser to have sufficient power, the length of the tube should not be less than 20 cm, while the required free spectral range for our purposes dictated a length of less than 32 cm.

With the above requirements in mind, the model was used to analyze the losses for a variable tube-to-grating distance by varying the tube length between 20 and 32 cm. The power was calculated according to Rigrod's equation for the power of a high gain laser,⁹ taking into account that the gain of the small signals is $g_0=2\text{ m}^{-1}$ (Ref. 10), the transmittance of the mirror $t_1=0.05$, and transmittance of the grating $t_2=1$. The results are presented in Fig. 2, in a normalized form, as P/P_s (P_s is the saturation power for a given λ).

As expected, the power increases with increasing WG tube length, as well as with decreasing distance between the mirror and the tube (when the dissipation of optical power reduces). Still, for certain configurations local power maxima are obtained. Namely, if the p -th and the first WG mode are in phase at the exit of the waveguide, the distribution of the field across the cross-section (perpendicular) plane is concentrated around the axis. This effect reduces dispersion in the free space, which reduces the overall optical power loss.

The choice of resonator dimensions was not guided only by the condition of maximum power, but also by the stability of the output. Stability is needed when

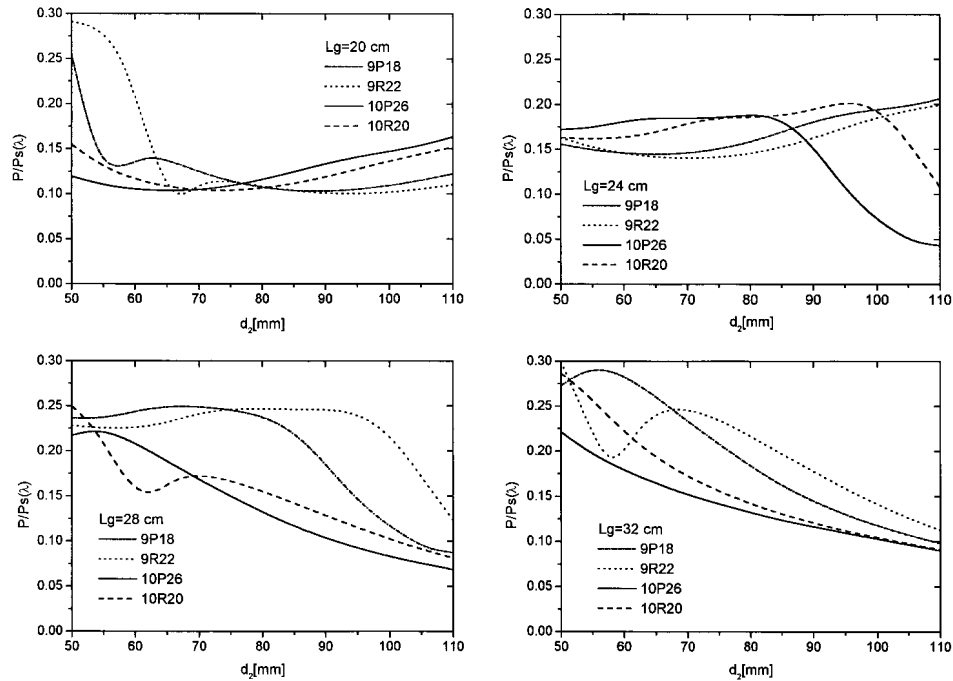


Fig. 2. Calculated values of the normalized laser power as a function of distance d_2 for four different laser emission lines.

the diffraction grating is rotated for emission line selection. Losses for various wavelengths, tube lengths and d_2 distances are given in Fig 2. It is observable that the power is less dependent on the tube length than on the d_2 distance. For tubes shorter than 25 cm, the power is stable for all modes, but is at low levels. Lengths of 28 cm and 32 cm have high instability. Thus, working lengths in the range from 24 cm to 26 were chosen as optimal.

A transversally monomode operation is ensured if the losses for mode EH₁₁ are at least 2 times lower than for the other modes. By choosing a resonator configuration that provides a somewhat lower power (relative to the power at $d_2=0$), stable laser operation is obtained. The configuration chosen, $l = 25.5$ cm, gives a power of P/P_s above 20 %, for all wavelengths. Also, this configuration for the optimal $d_2 = 6$ cm ensures that the difference between the losses of the fundamental and the higher modes exceeds 20 %, providing monomode operation. Good mode selectivity is also ensured for small deviations of d_2 . To increase the laser power for the laser lines of 9P and 9R branches the grating-to-tube distance can be increased to 11 cm. The latter configuration also ensures good mode structure (Fig. 3).

It should be noted that, in the calculations of output power, the parameters of low power signals g_0 and the saturation power were considered constant, although they depend on the resonator dimensions – they were actually larger for smaller values of a .

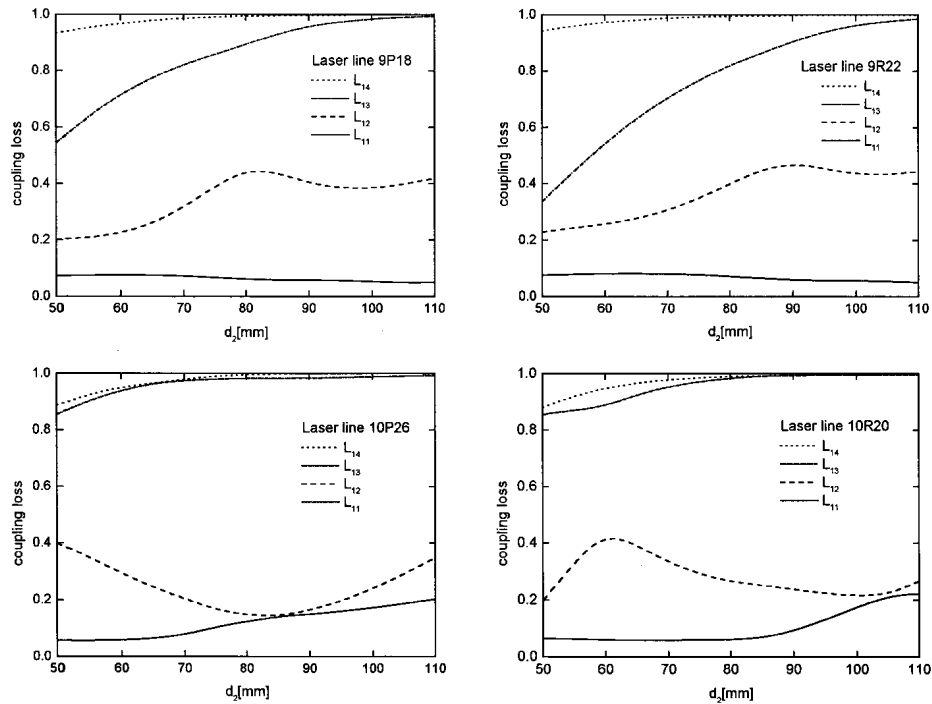


Fig. 3. The losses of four fundamental modes for $L_g = 25.5$ cm, and four different laser emission lines.

The calculation was performed for the chosen WG length of 25.5 cm, inner radius $a = 1.5$ mm, for all four laser emission branches (Fig. 4). On the basis of the mode coupling diagram, Fig. 3, and the power diagram, the optimal value of parameter d_2 was determined to be 6 cm.

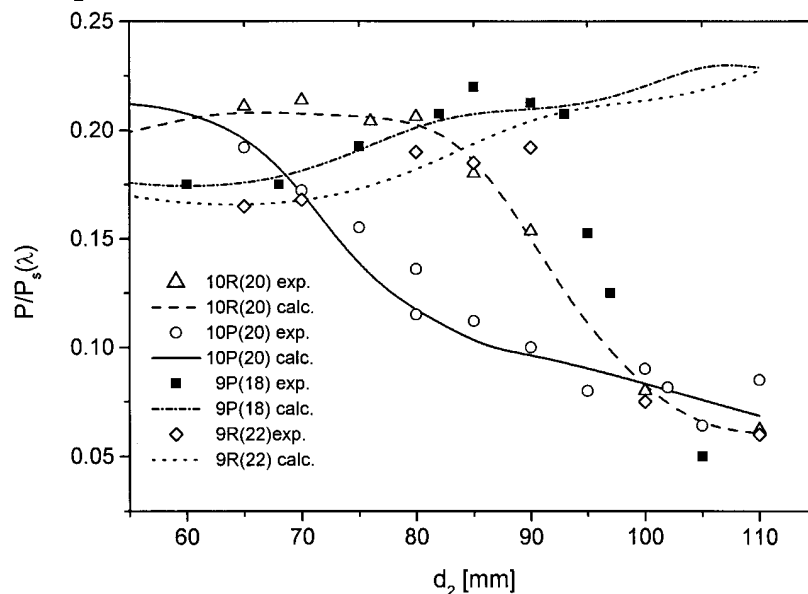


Fig. 4. Relative laser power as a function of waveguide-to-grating distance for a waveguide length of $L_g = 25.5$ cm, and four different emission line wavelengths.

LASER CONSTRUCTION

General construction

The above model and calculations were the basis for constructing the WG CO₂-laser presented in Fig. 5.

The laser consists of a water cooled quartz waveguide, inner dia. 3 mm, outer dia. 6 mm, length 25.5 cm, terminated by stainless steel electrodes. The discharge

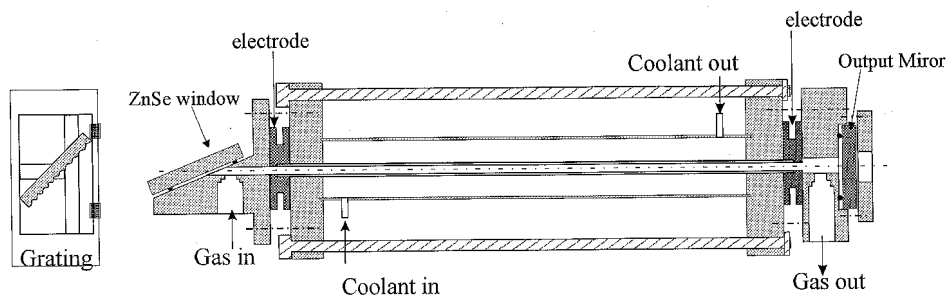


Fig. 5. Scheme of the laser.

is excited by high DC voltage, and the laser operates in the continuous wave regime. One end of the laser tube is terminated by a ZnSe Brewster window, and the other by a 5 % transmittance output coupling mirror.

The diffraction grating of 150 grooves/mm is placed on a separate mount. Its rotation serves for wavelength selection, and its transversal movement varies the laser resonator length. The optimal length varied between 30 cm and 37 cm, depending on the output emission wavelength. Wavelength selection and resonator length adjustment are done by coarse control of the grating mount. The grating mount is also finely positioned by a New Focus piezo positioner Model 8071, controlled by Multiaxis Picomotor Driver Model 8801, which is linked to a PC computer *via* a specially made TTL interface. We developed software for control of the positioner in C-language. The software communicates both with the piezo positioner and with the laser output power meter DigiRad Universal Laser Radiometer Model R-752, *via* an RS232 interface, and provides, upon request, either frequency stabilization or fine translational modifications of the resonator length (emission line scanning). Since the laser operates at pressures between 40 mbar and 120 mbar this enables scanning across 600 MHz within a typical emission line.

The laser is used in photoacoustic spectroscopy, where the obtained stability and tunability meet the most significant requirements.

Electrical current stabilization

Electrical current stabilization was applied to the electrical power supply system. Instead of using common ballast loads, which "consume" the supply voltage and place high requirements on the power supply, a special device was developed, which reduces current fluctuations to ± 0.5 %. The device is based on a high voltage VMOS transistor operating in the saturation regime.

The DC power supply provides high voltage at the laser electrodes. Without a ballast load in series with the laser, the laser operation cannot obtain stability, due to negative resistance of the discharge plasma. It was found that the minimum load required to compensate for the negative dynamic resistance of the laser is 400 k Ω . A change of the ballast load from 400 k Ω to 4 M Ω reduces the variations of the laser current from 24 % to 5 %, but at the same time increases the consumption of the power from 10 % to 50 %. A more practical solution is to utilize the dynamic resistance of non-linear active elements, like transistors, instead of passive ones. The authors of Ref. 11 proposed the use of a gas tube and BIP transistors. Our simpler solution with a VMOS transistor is presented in Fig. 6. The BUZ 90 VMOS transistor used has a break down voltage of 1000 V a high dynamic resistance and a gate current below 1 μ A.

Current stabilization was eventually achieved with a combination of a 400 k Ω ballast load and a BUZ 90 VMOS transistor working in the constant base voltage regime. The base potential can be adjusted for the saturation regime by a variable resistance. It has to be greater than V_{bmin} , where $V_{bmin} = I_{max} R_{source} + V_{gsth}$. The

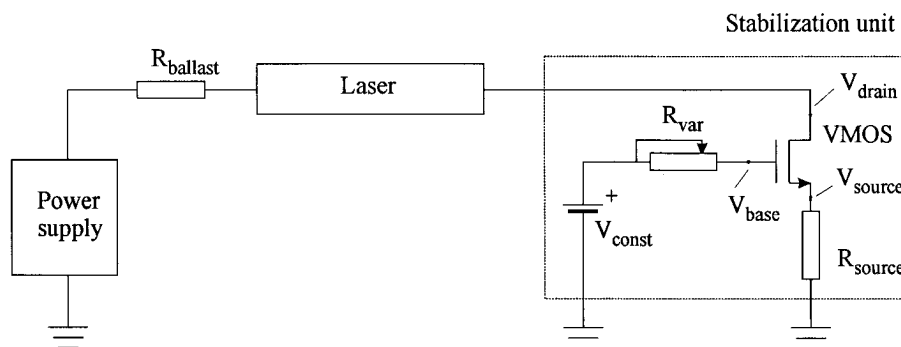


Fig. 6. Scheme of the high voltage current stabilized laser power supply.

stabilization module with a resistance $R_{\text{source}} = 3 \text{ k}\Omega$ reduces the laser current variation from 25 % to less than 1 %. Increasing R_{source} improves current stabilization, but also increases the probability of transistor break down, and requires higher base voltages.

EXPERIMENTAL TEST

In operation, the laser works at about 50 emission lines, with a typical output power ranging from 100 to 500 mW. The DC voltage applied on the ballast loads and the laser is typically 10 kV at 40 mbar of the gas mixture. The beam cross section has good radial symmetry.

The laser operation was tested at several typical emission lines of all 4 branches of the emission spectrum as a function of distance d_2 , and compared to the theoretical predictions of the model. The results are presented in Fig. 5 for the lines 10R(20), 10P(20), 9P(18) and 9R(22). Very good agreement was obtained in both branches of the 10.6 μm band. Good agreement was also obtained for the branches 9P and 9R, at distances $d_2 < 95 \text{ mm}$. At greater values of d_2 the real laser power drops sharply, which does not agree with the results of the modeling. However, temporary construction imperfections are a very likely cause of this discrepancy. The discrepancy, on the other hand, does not impede spectroscopic work with the laser at all, since it can be reliably operated at $d_2 < 95 \text{ mm}$.

CONCLUSION

A theoretical laser mode coupling model, in the form of a computer simulation program, was made to optimize the parameters of a waveguide CO_2 -laser for use in photoacoustic spectroscopy of gases. The design requirements included placement of a terminal diffraction grating outside the laser tube, which meant considerable intracavity free space outside the waveguide. The results of the optimization were: a waveguide tube of 25.5 cm length and 3 mm inner diameter, and a variable tube-to-grating distance in the range 6 cm to 9 cm.

A CW waveguide CO_2 -laser was designed and built according to the modeling results around a water cooled quartz waveguide. The laser current was stabilized with $\pm 0.5 \%$ tolerance by a self-made device that included a VMOS transistor, which proved to be a simpler and lower-cost solution than a combination of classical gas tubes and BIP transistors.

The laser operation (output powers in the range 100 mW to 500 mW) proved to be in good agreement with the predictions, especially for the 10.6 μm emission band.

ИЗВОД

ТАЛАСОВОДНИ СО₂-ЛАСЕР ЗА ФОТОАКУСТИЧКУ СПЕКТРОСКОПИЈУ ГАСОВА

ГОРДАНА М. ОСТОЈИЋ, БОЈАН Б. РАДАК И ЉУБИЦА Т. ПЕТКОВСКА

Институт за нуклеарне науке "Винча", Лабораторија за физичку хемију, бр. 522, 11001 Београд

Направљен је теоријски модел таласоводног СО₂-ласера ради оптимизације димензија таласовода и резонатора ласера, тј. добијања најбоље модне структуре уз максимизирање излазне снаге. Резултати су употребљени за конструкцију и израду ласера око кварцног таласовода дужине 25,5 cm и унутрашњег пречника 3 mm. Једноставна, економична и ефикасна стабилизација струје ласера је изведена, заснована на VMOS технологији, која је обезбедила стабилизацију струје у границама $\pm 0,5\%$. Избором радне фреквенције ласера и/или стабилизацијом фреквенције управљало се помоћу пиезо микро позиционера, који је био спрегнут са мерачем снаге преко РС рачунара и покретан самостално развијеним софтвером. Експериментални тест изграђеног ласера је показао добро слагање са моделом.

(Примљено 27. октобра 1999, ревидирано 25. фебруара 2000)

REFERENCES

1. Lj. T. Petkovska, Š. S. Miljanić, *Infrared Phys. Technol.* **34** (1997) 331
2. B. B. Radak, I. Pastirk, G. Ristić, Lj. Petkovska, *Infrared Phys. Technol.* **39** (1998) 7
3. Lj. T. Petkovska, M. S. Trtica, M. M. Stojiljković, G. S. Ristić, Š. S. Miljanić, *J. Quant. Spectrosc. Radiat. Transfer* **54** (1995) 509
4. Lj. T. Petkovska, B. B. Radak, Š. S. Miljanić, R. T. Bailey, F. R. Cruickshank, D. Pugh, *Proc. Indian Acad. Sci. (Chem. Sci.)* **103** (1991) 401
5. R. L. Abrams, A. N. Chester, *Appl. Optics* **13** (1974) 2117
6. R. Gerlach, W. Dianyan, M. M. Amer, *IEEE J. Quant. Elect.* **20** (1984) 948
7. B. Schröder, *IEEE J. Quant. Elect.* **27** (1991) 158
8. J. Henningsen, M. Hammerich, A. Olafsson, *Appl. Phys.* **B 51** (1990) 272
9. W. W. Rigrod, *J. Appl. Phys.* **36** (1965) 2487
10. N. Ioli, V. Panchenko, M. Pellegrino, F. Strumia, *Appl. Phys.* **B 38** (1985) 23
11. M. J. Posakony, *Rev. Sci. Instrum.* **43** (1972) 270.